

# Dysprosium Activated $\text{Sr}_3\text{Al}_2\text{O}_6$ Nanophosphor for Display Device Applications

Chitra M<sup>\*1</sup>, Ananda kumari R<sup>2</sup> and Nagaraju G<sup>3</sup>

<sup>1</sup>Sree Siddaganga Research and Development Centre, Tumkur university, Tumkur, India. chitramallela@gmail.com

<sup>2</sup>Sree Siddaganga college of Arts, Science and Commerce, Tumkur, India. janandakumari@gmail.com

<sup>3</sup>Department of Chemistry, Sree Siddaganga Institute of Technology, Tumkur, India. nagarajugn@gmail.com

**Abstract:** Phosphor powders of Strontium aluminate doped with 1, 3, 5, 7, 9 and 11 molar concentrations of  $\text{Dy}^{3+}$  were synthesized by Urea assisted solution combustion method. Structural characteristics of calcined phosphors have been carried out employing the techniques such as X-ray diffraction, Scanning electron microscope with Energy dispersive X-ray analysis. The phosphors have cubic structure. Average crystallite size estimated using Debye-Scherrer's formula was around 31 nm. Fourier infrared spectral peak at  $868\text{ cm}^{-1}$  was attributed to Sr-Al ligand. The porous nature of phosphors was noticed in Scanning electron micrographs. The nanostructure of the phosphors was confirmed by Transmission electron microscopic studies. The range of band gap energies found from Kubelka-Munk plots of the Diffused reflectance Spectra was 5.52 eV to 5.64 eV. Emission peaks from Photoluminescence studies results at 479 nm, 574 nm & 676 nm upon excitation with 240 nm, 289 nm & 340 nm UV light respectively. Excellent white light emission from combustion synthesized nanophosphors has been justified by the chromaticity diagram. The average temperature related to color of light emitted by the phosphors was found to be  $4314\text{ }^\circ\text{K}$ .

**Index Terms:** Combustion synthesis, Chromaticity diagram (CIE), Color correlated temperature (CCT), Diffused reflectance (DRS), Energy dispersive X-ray analysis (EDAX), Fourier transform Infra red (FTIR) spectra, Powder X-ray diffraction (PXRD), Photoluminescence(PL), Scanning electron microscope (SEM), Transmission electron microscope (TEM).

## I. INTRODUCTION

In recent years, highly luminescent inorganic nano phosphors activated by rare earth ions have gained importance. (Jing Li et.al.2012; Dongli wi et al., 2009). The alkaline-earth- rare-earth (Ce, Tb, Dy..) doped Aluminate systems form a strong base for fluorescent lamp and plasma display phosphors as these materials can absorb, store and gradually release energy in the form of visible light (Song H. et al., 2008).  $\text{SrAl}_2\text{O}_4$ , a binary

alkaline earth aluminate (Palilla F.C et al., 1968; Poort S.H.M, 1995) is one of the typical matrices for long-duration luminescent materials. It is an appropriate host lattice with a wide band emission (Zuoling F., et al., 2005). In addition, Strontium aluminate phosphor is more stable than sulphide phosphors.  $\text{Dy}^{3+}$  is one of the most widely used rare-earth ion activators for preparing blue, yellow and red light emitting luminescent materials and in making tricolor energy saving fluorescent lamps (Li F. et al., 2017; Basavaraj R.B. et al., 2017; Basavaraj R.B et al., 2015). For example:  $\text{Eu}^{2+}$  doped  $\text{SrAl}_2\text{O}_4$  exhibit strong and long persistent luminescence in green region (Peng T. et al., 2004).  $\text{SrAl}_2\text{O}_4$ ;  $\text{Eu}^{2+}$ ,  $\text{Dy}^{3+}$  (Matsuzawa T. et al., 1996; Yang P. 2002) and  $\text{Sr}_4\text{Al}_{14}\text{O}_{25}$ ;  $\text{Eu}^{2+}$ ,  $\text{Dy}^{3+}$  (Matsuzawa T. et al., 1996) have been widely studied for possible applications in emerging lighting field. Of late, another form  $\text{Sr}_3\text{Al}_2\text{O}_6$  has also attracted interests of many researchers (Katsumath T. et al., 1996; Pan Y. et al., 2006; Liu Y & Xu C.N, 2000; Akiyama M. et al., 1998).

As compared with other synthesis methods such as solid state reaction method (Rao R.P., 1994), co-precipitation (Lin Y.H. et al.), sol-gel method (Kurihara L.K. & Suib S.I., 1993; Peng T.Y. et al., 2004) hydrothermal method (Sun X.M, Liu J.F., & Li Y.D., 2006; Zhu H.L. et al., 2005; Titirichi M.M., Antoniett M. & Thomas A., 2006), reverse micro-emulsion method etc., the solution combustion synthesis (SCS) is widely used in the synthesis and processing of various materials namely composites, catalysts, ceramics, nanomaterials etc., as it is one step, energy saving and fast (Huajie S., & Donghua C., 2007; Barros B.S. et al, 2006 ; Patil K.C. et al., 2002). This method utilizes simple equipment to prepare high purity products. It also facilitates the stabilization of metastable phases and the formation of products with different shapes and sizes (Kashinath C.Patil, Aruna S.T., & Tanu mimani, 2002).

\* Corresponding Author

Present paper is concerned with the combustion synthesis and systematic study of  $\text{Dy}^{3+}$  activated  $\text{Sr}_3\text{Al}_2\text{O}_6$  (SAL) Nanophosphors (Nps.). The photometric studies such as DRS & PL were carried out on the combustion synthesized nanophosphors. CIE co-ordinates & CCT were evaluated to find their potential applicability in solid state lighting field.

## II. MATERIALS & METHODS

The stoichiometric quantities of Strontium nitrate [ $\text{Sr}(\text{NO}_3)_2$ ], Aluminium nitrate nonahydrate [ $\text{Al}(\text{NO}_3)_3 \cdot 9\text{H}_2\text{O}$ ], Dysprosium nitrate [ $\text{Dy}(\text{NO}_3)_3 \cdot 6\text{H}_2\text{O}$ ] and Urea [ $\text{CO}(\text{NH}_2)_2$ ] of 99.9% purity (Sigma Aldrich) were dissolved in deionized water. The contents were continuously stirred till a homogeneous solution was obtained. This solution was placed in a Muffle furnace heated to  $500^\circ\text{C}$  previously. The solution has undergone combustion and a white foamy and voluminous Strontium aluminate ash was obtained in about 5 min. The ash after cooling to room temperature, made to a fine powder and then calcined at  $950^\circ\text{C}$ .

Rigaku smart lab X-ray diffractometer was used to find the Phase purity and crystallinity of the powders. Perkin Elmer Spectrophotometer was used for Infrared spectral studies. Tescan Vega3 LMU having a magnification upto 10,00000X and a resolution of 3 nm was used for SEM and EDAX studies. TEM, Hitachi H-8100 was used to confirm the crystallite size obtained from Debye-Scherrer's formula. LABINDIA UV-VIS Spectrophotometer UV33092 was used to obtain DRS of the powders. The Agilent Technologies Cary Eclipse Fluorescence spectrophotometer operational with Xenon lamp was used for PL measurement.

## III. RESULTS & DISCUSSION

### A. X-ray diffraction studies

"Fig.1"(a)-(f) shows XRD patterns of  $\text{Dy}^{3+}$  activated Strontium aluminate powders calcined at  $950^\circ\text{C}$ . The positions of the peaks corresponded entirely with standard PDF card no.24-1187 and were indexed to a cubic phase  $\text{Sr}_3\text{Al}_2\text{O}_6$  with a space group  $\text{Pa}_3$  (205) (Chengkang Chang et al., 2010). The average crystallite sizes of the powders were determined using Debye – Scherrer's equation:

$$D = k\lambda/\beta\cos\theta\text{-----Eqn. (1)}$$

Here  $k= 0.9$

$\beta$  = full width at half maximum (FWHM in radian)

$\lambda$  = wavelength of X-rays

$\theta$  = Bragg's angle of diffraction

The average crystallite sizes and Lattice strain values are tabulated in "Table I".

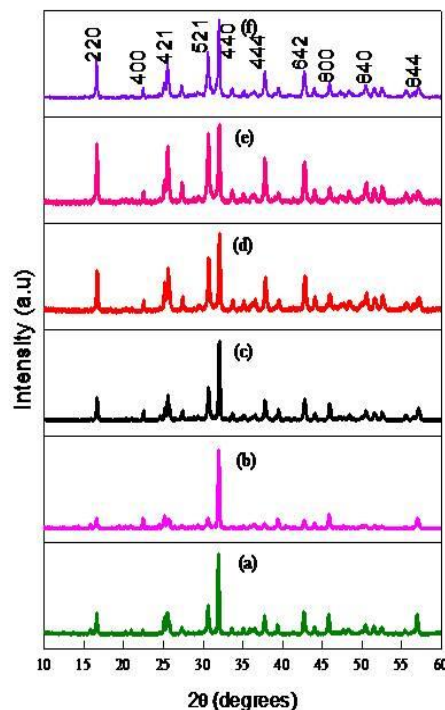


Fig.1(a)-(f). PXRD patterns of SAL: (1, 3, 5, 7, 9 & 11) mol%  $\text{Dy}^{3+}$  Powders.

Table I. The crystallite sizes & Lattice Strain values of SAL: (1, 3, 5, 7, 9 & 11) mol%  $\text{Dy}^{3+}$  Nps.

$\text{Dy}^{3+}$ (mol%)	Crystallite size (nm) Scherrer's equation	Energy gap( $E_g$ ) (eV)	Lattice Strain ( $10^{-3}$ )
1	34	5.52	4.1
3	32	5.58	4.11
5	31	5.59	4.19
7	30	5.60	4.90
9	29	5.62	4.95
11	27	5.64	4.98

### B. Fourier infrared spectral studies

"Fig.2" (a-f) shows the FTIR spectra of the nano Phosphors in the range  $500$  to  $4000\text{ cm}^{-1}$  wavenumber. From FTIR it is also observed that most of the peaks are due to Sr-O, Al-O and O-H stretching frequencies. The peak at  $3625\text{ cm}^{-1}$  is due to stretching frequencies of  $\text{AlO}_4$  group.  $\text{OH}^-$  stretching vibrations of hydroxyl groups have answered for broad band at  $3482\text{ cm}^{-1}$ . The peaks at  $687\text{ cm}^{-1}$  and  $786\text{ cm}^{-1}$  represent the vibrations of Al-O, while the peak at  $721\text{ cm}^{-1}$  is ascribed to Sr-O groups. The peaks appeared at  $951$ ,  $1028$  &  $1100\text{ cm}^{-1}$  are characteristic of the anti-symmetric stretching ( $\text{V}_3$  region) of Sr-O bond (Angappan.S., Bechermans L.J. & Augustin C.O., 2004).

However, weak absorption peaks at  $1628$  and  $1772\text{ cm}^{-1}$

appear due to bending vibrations and asymmetric stretch of absorbed water molecule from the atmosphere. A distinct shoulder of absorbed water molecule is also observed at  $2482\text{ cm}^{-1}$  (Maaylee Stomp et al., 2007). The phosphors under study showed a characteristic peak of Strontium aluminate at  $868\text{ cm}^{-1}$  (Lu C.H., Chen S.Y., & Hsu C.H., 2007). The peak at  $1476\text{ cm}^{-1}$  is ascribed to the vibrations of C-O bond.

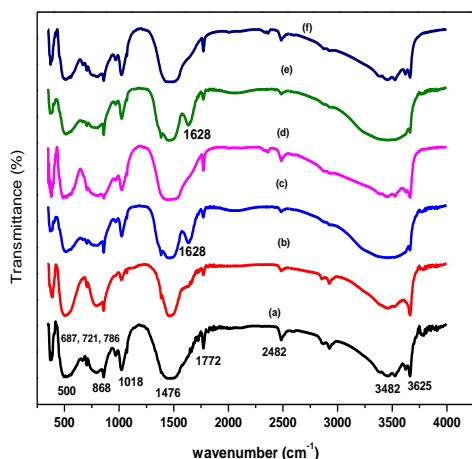


Fig.2 (a)-(f). Transmittance spectra of SAL: (1, 3, 5, 7, 9 & 11) mol%  $\text{Dy}^{3+}$  Nps.

### C. Scanning electron microscope studies

“Figs.3” (a)-(f) show the Scanning electron (SEM) images of (1, 3, 5, 7, 9 & 11) mol%  $\text{Dy}^{3+}$  activated SAL nanophosphors at different magnifications. The particles were found to have different shapes and sizes (highlighted by yellow colored circles). The images also exhibited pores and voids formed by escaping gases during combustion. The images indicate the impact of  $\text{Dy}^{3+}$  concentration on morphology of the phosphors. The crystallites have sizes within 50 nm.

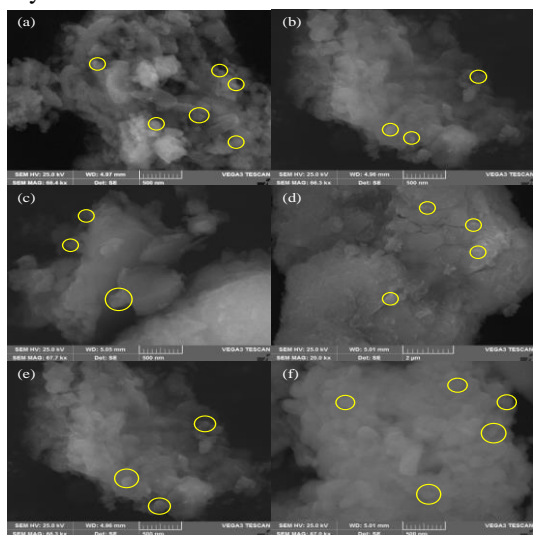


Fig.3(a)-(f). SEM images of SAL: (1, 3, 5, 7, 9 & 11) mol%  $\text{Dy}^{3+}$  Nps.

### D. Energy dispersive X-ray with SEM studies

The EDAX spectrum of SAL: 7 mol%  $\text{Dy}^{3+}$  nanophosphor shown in “Fig.4” identifies and quantifies its elemental composition in a small portion of its SEM image (inset) whose area is of the order of nanometers. The characteristic X-ray emissions of Sr, Al, O & Dy were observed. The elemental composition in the table (inset) indicates the presence of  $\text{Dy}^{3+}$  ions in the host. Further, it was observed that nanometer-sized particles were uniformly distributed in the synthesized nanophosphors.

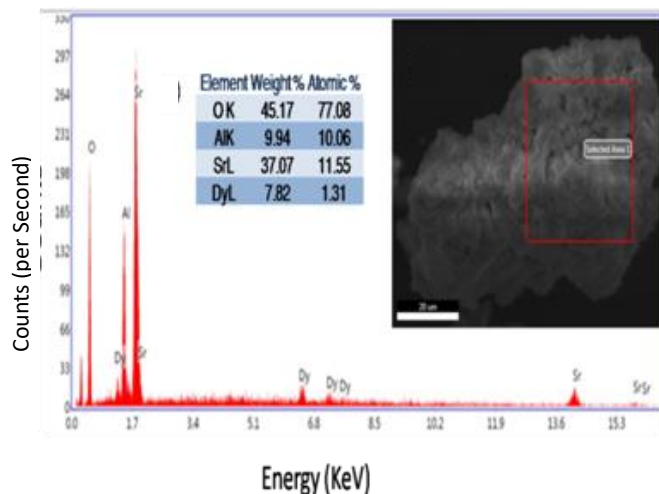


Fig.4. EDAX of SAL: 7 mol%  $\text{Dy}^{3+}$  Np.

### E. Transmission electron microscope studies

“Fig.5” (a) shows the TEM image of a particle of SAL: 7 mol%  $\text{Dy}^{3+}$  nanophosphor calcinated at  $950^\circ\text{C}$ . Its size is of the order of 50 nm. HRTEM image shown in “Fig.5” (b) depicts the interplanar distance ‘d’ between (440) & (444) planes as 0.24 nm. The inset SAED pattern reveals an irregular spherical morphology of the particle.

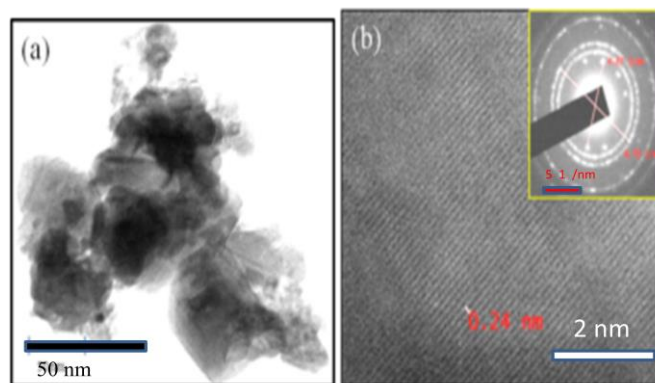


Fig.5. (a) TEM & (b) HRTEM images of calcined SAL: 7 mol%  $\text{Dy}^{3+}$  Np. (inset: SAED pattern).

F. Diffused reflectance studies

“Fig.6” (a)-(f) & “Fig.7” (a)-(f) show DRS and Kubelka-Munk plots for band gap energies (Darshan G.P. et al., 2016) of the prepared nanophosphors. The DRS spectra exhibited peaks at 266 nm & 366 nm that were due to  ${}^6H_{15/2} \rightarrow {}^4I_{7/2}$  and  ${}^6H_{15/2} \rightarrow {}^4I_{11/2}$  transitions. For higher concentrations of  $Dy^{3+}$ , additional weak absorption peaks at 752 nm & 806 nm due to  ${}^6H_{15/2} \rightarrow {}^6F_{5/2}$  &  ${}^6H_{15/2} \rightarrow {}^6F_{7/2}$  transitions were obtained (Tsunekawa S. et al., 2003). The optical band gap (direct) energy values tabulated in “Table I” were in the range 5.52eV - 5.64eV (Jisha V.T., & Saji kumar A.C., 2016). The increase in bandgap energies with increase in concentration of Dysprosium can be attributed to the decrease in its crystallite size. “Fig.8” depicts the variation in band gap energy values with  $Dy^{3+}$  ion concentration. The increase in concentration of Dysprosium ion as well as change in crystallite size has resulted in red shifting of the DRS bands.

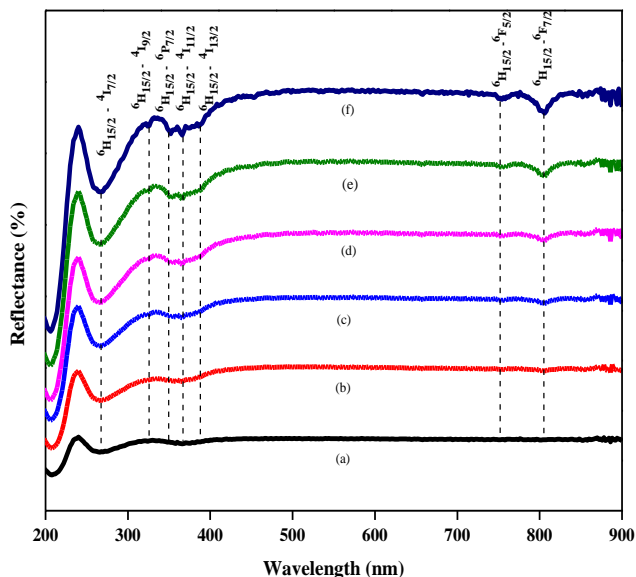


Fig.6(a)-(f). Diffused reflectance spectra of SAL: (1, 3, 5, 9 & 11) mol%  $Dy^{3+}$  Nps.

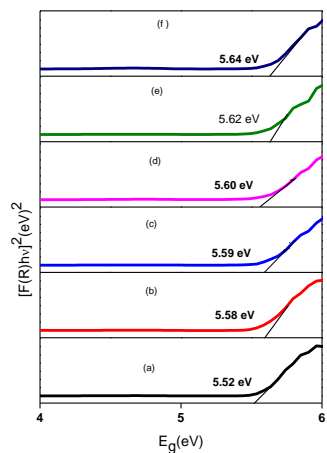


Fig.7 (a)-(f) Kubelka-Munk plots of SAL: (1, 3, 5, 7, 9 & 11) mol%  $Dy^{3+}$  Nps.

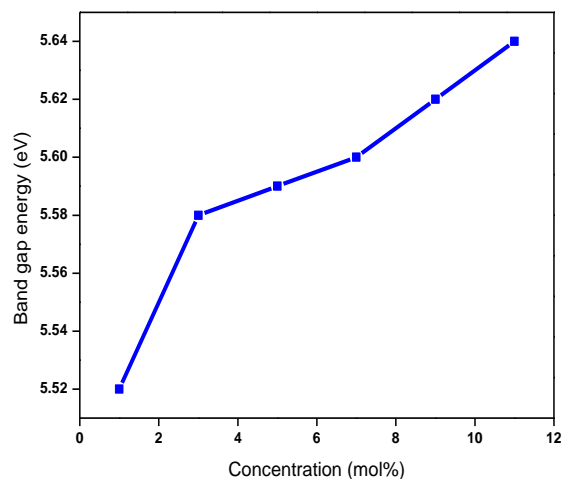


Fig.8. Variation in Bandgap Energies with  $Dy^{3+}$  ion concentration

G. Photoluminescence studies

“Fig.9 (a)” shows excitation peaks at 240 nm, 289 nm & 340 nm when monitored at emission wavelengths 479 nm, 574 nm and 676 nm respectively. Transitions  ${}^4F_{9/2} \rightarrow {}^6H_{15/2}$  (blue),  ${}^4F_{9/2} \rightarrow {}^6H_{13/2}$  (Yellow) &  ${}^4F_{9/2} \rightarrow {}^6H_{11/2}$  (Red) give rise to emission peaks of 1, 3, 5, 7, 9 & 11 mol%  $Dy^{3+}$  doped SAL phosphors at 479 nm (Blue), 574 nm (Yellow) and 676 nm (Red) as shown in “Fig.9” (b) (Ishwar Prasad Sahu, D. P. Bisen et.al.,2005; Abanti Nag & Narayanan Kutty T. R., 2003; Liu B., Shi C.S., & Qi Z.M., 2005; Omkaram I. & Buddhudu S., 2009; You P.L. et al., 2011; Liu B., Kong L.J., & Shi C.S., 2007; Chen Y.H. et al., 2009; Kuang J.Y., Liu Y.L., & Zhang J.X., 2006). The characteristic emission of light confirms that  $Dy^{3+}$  ions act as luminescent centers in  $Sr_3Al_2O_6$  nanophosphor.

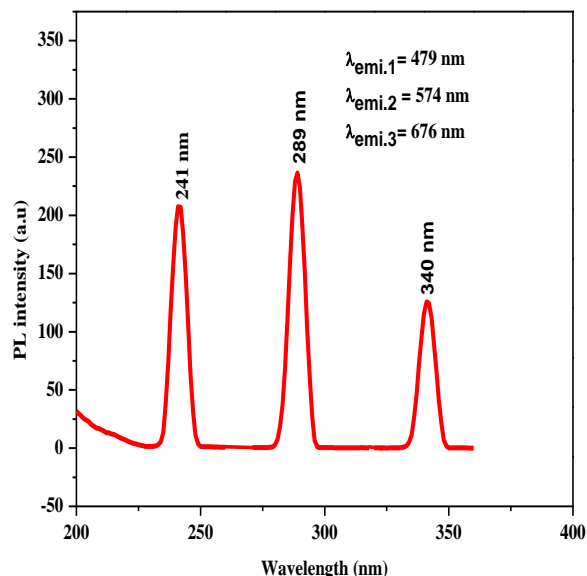


Fig. 9 (a) Excitation spectra SAL: (1) mol%  $Dy^{3+}$  Nps.

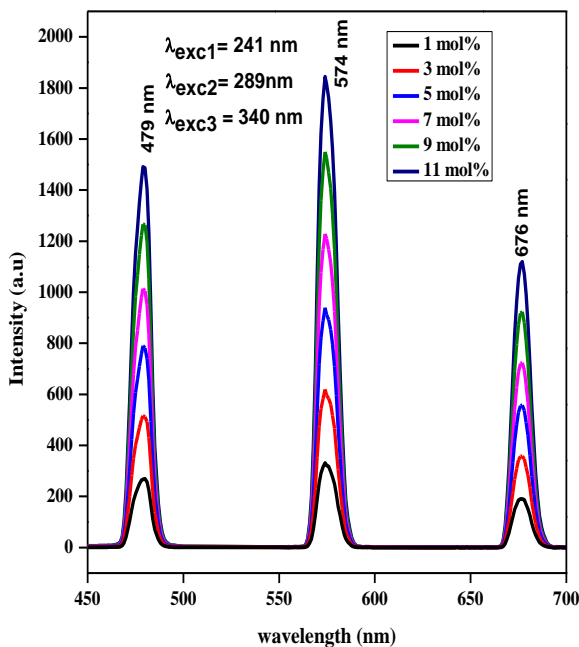


Fig. 9(b) Emission spectra of SAL : (1, 3, 5,7, 9 & 11) mol% Dy<sup>3+</sup> Nps.

The luminescence color of phosphors excited under 240 nm, 289 nm & 340 nm has been characterized by the chromaticity diagram (CIE (1931) International Commission on Illumination. Publication CIE No. 15) shown in “Fig.10 (a)”. The evaluated CIE co-ordinates (inset table) of all phosphors, placed almost at (x = 0.37, y = 0.38) were disposed in ‘chromatic shoe’. Luminescent colors of all phosphors were represented by the colored dots in the white region of the chromaticity diagram. To identify the technical applicability of this white light emission, correlated color temperature (CCT) was determined from CIE coordinates “Fig.10 (b)” shows the CCT diagram of SAL: Dy<sup>3+</sup> (1-11) mol % (McCamy C.S, 1992). CCT co-ordinates were found from “Eqns. (2) and (3)”.

$$U' = 4x / -2x + 12y + 3 \text{ ----- Eqn. (2)}$$

$$V' = 9y / -2x + 12y + 3 \text{ ----- Eqn. (3)}$$

The average CCT of SAL: Dy<sup>3+</sup> phosphors was found to be 4314° K.

**CONCLUSION**

The phosphors of Sr<sub>3</sub>Al<sub>2</sub>O<sub>6</sub>: (1, 3, 5, 7, 9 & 11) mol% Dy<sup>3+</sup> were synthesized by fast, simple and one-step solution combustion method. The XRD analysis confirmed the face centered cubic crystal structure for the phosphors with their crystallite sizes in nanometer range. FTIR spectra confirmed the formation & crystallization of Strontium aluminate. The EDAX with SEM confirmed the composition of Sr<sub>3</sub>Al<sub>2</sub>O<sub>6</sub>: Dy<sup>3+</sup> (Sr, Al, O and Dy) & uniform distribution of Dy<sup>3+</sup> in host lattice. As shown by SEM images, the particles were found to have acquired a regular shape at higher concentration of the activator Dy<sup>3+</sup>. The photoluminescence emission spectra of 1, 3, 5, 7, 9 & 11 molar concentration Dy<sup>3+</sup> activated Sr<sub>3</sub>Al<sub>2</sub>O<sub>6</sub> nano phosphors displayed a characteristic white light emission. Increase in

concentration of Dy<sup>3+</sup> has enhanced the illumination intensity. The CCT for all the six nanophosphors was in the range 4105°K - 4507°K which was well within the daylight temperature. Excellent emission of white light from all concentrations of Dy doped Sr<sub>3</sub>Al<sub>2</sub>O<sub>6</sub> nanophosphors indicates their possible application in display devices.

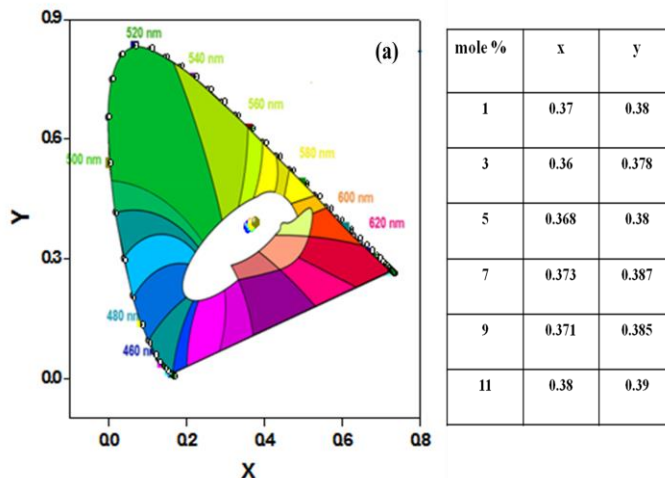


Fig.10. (a) CIE chromaticity diagram with a table of color co-ordinates x & y for SAL: (1, 3, 5, 7, 9 & 11) mol% Dy<sup>3+</sup> Nps.

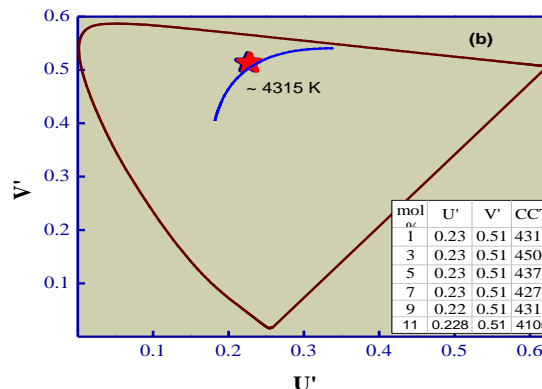


Fig. 10(b) CCT diagram for SAL: (1, 3, 5, 7, 9 & 11) mol% Dy<sup>3+</sup> Nps.

**ACKNOWLEDGMENTS**

This work was fully supported by Chemistry Research Centre, Sree Siddaganga Institute of Technology, Tumkur. The authors would like to thank CNR Rao center for nanomaterials, Tumkur university, Tumkur, Dr.K.V.R. Murthy, MSU, Baroda.

**REFERENCES**

Jing Li., Jiyang Wang., Shujuan Han., Yongjie Guo., & Yongzheng Wang. (2012), *J. Rare Earths.* 30, pp.967-971.  
 Donglei Wei., Yanlin Huang., Liang SHI., Xuebin Qiao. & Hyo Jin Seo. (2009), *J. Rare Earths.* 27, pp. 905-910.  
 Song H., Chen D., Tang W. & Peng Y. (2008), *Displays* 29, pp. 41-44.



- Palilla F.C., Levine A.K., & Tomkus M.R. (1968), Fluorescent properties of alkaline earth aluminates of the type MAI<sub>2</sub>O<sub>4</sub> activated by divalent europium, *J. Electrochem. Soc.* 115, pp. 642-644.
- Poort S.H.M., Blokpoel W.P., & Blasse G. (1995), Luminescence of Eu<sup>2+</sup> in barium and strontium aluminate and gallate, *Chem. Mater.* 7, pp.1547-1551.
- Zuoling F., Shihong Z., & Siyuan Z. (2005), *J. Phys. Chem. B.*, 109, pp.14396-14400.
- Li F., Liu SQ., Qi RY., Li H., & Cui TF. (2017), Effective visualization of latent fingerprints with red fluorescent La<sub>2</sub>(MoO<sub>4</sub>)<sub>3</sub>:Eu<sup>3+</sup> microcrystals. *J. Alloys Compd.*, 727, pp. 924.
- Basavaraj R.B., Nagabhushana H., Daruka Prasad B., & Vijayakumar G.R. (2017), Zinc silicates with tunable morphology by surfactant assisted sonochemical route suitable for NUV excitable white light emitting diodes. *Ultrason Sonochem.*, 34, pp.700.
- Basavaraj R.B., Nagabhushana H., Daruka Prasad B., Sharma S.C., Prashantha S.C., Nagabhushana B.M. (2015), A single host white light emitting Zn<sub>2</sub>SiO<sub>4</sub>:Re<sup>3+</sup> (Eu, Dy, Sm) phosphor for LED applications. *Optik.*, 126, pp.1745.
- Peng T., Yang H., Pu X., Hu B., Jiang Z., & Yan.C. (2004), Combustion synthesis and photoluminescence of SrAl<sub>2</sub>O<sub>4</sub>:Eu, Dy phosphor nanoparticles, *Mater. Lett.* 58, pp.352-356.
- Matsuzawa T., Aoki Y., Takeuchi T., & Murayama Y. (1996), *J. Electrochem. Soc.* 143, pp.2670.
- Yang P., Lu M.K., Song C.F., Xu D., Yuan D.R., Xia G.M. & Liu Inorg S.W. (2002) *Chem. Commun.* 5(3), pp. 919.
- Matsuzawa T., Aoki Y., Takeuchi T. & Murayama Y. (1996) *J. Electrochem. Soc.* 143, pp. 2670.
- Katsumatha T., Sasajima K., Nabae T., Kumuro S. & Morikawa T. (1996) *J. Am. Ceram. Soc.* 81 (2), pp. 413.
- Pan Y., Sung H., Wu H., Wang J., Yang X., Wu M., & Su Q. (2006), *Mater. Res. Bull.* 41, pp.225.
- Liu Y. & Xu C.N. (2003), *J. Phys. Chem. B* 107(17), pp.3991.
- Akiyama M., Xu C.N., Nonaka k. & Watanabe T. (1998) *Appl. Phys. Lett.* 73, pp.3046.
- Rao R.P. (1994), *J. Electrochem. Soc.* 143, pp.189.
- Lin Y.H., Zhang Z.T., Zhang F., Tang Z.I. & Chen Q.M. (2000) *Mater. Chem. Phys.* 65, pp.103.
- Kurihara L.K. & Suib S.I. (1993) *Chem. Mater.* 5, 609.
- Peng T.Y., Liu H.J., Yang H.P. & Yan C.H. (2004) *Mater. Chem. Phys.* 85, pp.68.
- Sun X.M., Liu J.F. & Li Y.D. (2006) *Chem. Mater.* 18, pp.3486.
- Zhu H.L., Yao K.H., Zhang H. & Yang D.R. (2005), *J. Phys. Chem.* B109, pp.20676.
- Titirici M.M., Antonietti M. & Thomas A. (2006), *Chem. Mater.* 18, pp.3808.
- Huajie S., & Donghua C. (2007), *Luminescence*; 22, pp.554-558.
- Barros B. S., Melo P.S., Kiminami R. H.G.A., Costa A. C. F. M., de Sá G.A., & Alves Jr. S. (2006), *J. Mater. Sci.*, 41, pp. 4744-4748.
- Patil K.C., Aruna S.T., In: Borisov AA., De Luca LT., Merzhanov AG. & Schek YN. (2002), Redox methods in SHS Practice in self-propagating high temperature synthesis of materials, New York: T&F; Collection of 17 articles by experts in the area reflecting the trends in SHS coercing theory and practice of combustion, material synthesis and applications.
- Kashinath C. Patil., Aruna S.T. & Tanu mimani. (2002) current opinion in solid state and Materials science 6, pp. 507- 512.
- Chengkang Chang., Wen Li., Xiaojun Huang., Zhiyu Wang., Xi Chen., Xi Qian. & Rui Guo. (2010), *J. Luminescence* 130, pp. 347-350.
- Angappan S., Bechermans L.J. & Augustin C.O. (2004), *Mater. Lett.* 58, pp. 2283.
- Maaylee Stomp, Jef Huisman, Lucas j Stal, Hans C.P, Matthij S (2007) ISME journal 1(4)-271-282.
- Lu C.H., Chen S.Y. & Hsu C.H. (2007), *Mater. Sci. Engg. B* 140, pp.218.
- Darshan G. P., Premkumar H.B., Nagabhushana H., Sharma S.C., Daruka Prasad B. & Prashantha S.C. (2016) Neodymium doped yttrium aluminate synthesis and optical properties—A blue light emitting nanophosphor and its use in advanced forensic analysis. *Dyes Pigm.* 134, pp. 227.
- Tsunekawa S., Wang J., Kawazoe Y., & Kasuya A. (2003), Blue shifts in the ultraviolet absorption spectra of cerium oxide nanocrystallites. *J Appl Phys.* 94, pp. 3654.
- Jisha V.T., & Saji kumar A.C. (2016), *Ultra Scientist Vol.* 28(4) B, pp. 88-93.
- Chroma M., Pinkas J., Pakutinskiene I., Beganskiene A., & Kareiva A. (2005), *Ceram. Int.* 31, pp.1123.
- Abanti Nag., & Narayanan Kutty T. R. (2003), *J. Mater. Chem.*, 13, pp. 370.
- Liu B., Shi C.S., & Qi Z.M. (2005), *Appl. Phys. Lett.* 86, pp. 191111.
- Omkaram I., & Buddhudu S. (2009), *Opt. Mater.* 32, pp.8.
- You P.L., Yin G.F., Chen X.C., Yue B., Huang Z., Liao X., & Yao Y. (2011) *Opt. Mater.* 33, pp.1808.
- Liu B., Kong L.J., & Shi C.S. (2007), *J. Lumin.* 122–12, pp. 121.
- Chen Y.H., Cheng X.R., Liu M., Qi Z.M., & Shi C.S. (2009), *J. Lumin.* 129, pp.531.
- Kuang J.Y., Liu Y.L., & Zhang J.X. (2006), *J. Solid State Chem.* 179, pp. 266.
- CIE (1931) *International Commission on Illumination.* publication, CIE No. 15 (E-1.3.1).
- McCamy C.S. (1992), Correlated color temperature as an explicit function of chromaticity coordinates, *Color Res. Appl.* 17, pp.142-144.

\*\*\*